Third International Conference on Sustainable Construction Materials and Technologies http://www.claisse.info/Proceedings.htm

Effect of microstructure and moisture content on the electric conductivity of hardened cement paste

Kiyofumi Kurumisawa[1,*] and Toyoharu Nawa[2]

[1] *Faculty of engineering, Hokkaido University, Japan*
Kita 13, Nishi 8, Kita-ku, Sapporo, Hokkaido, 060-8628, kurumi@eng.hokudai.ac.jp
[2] *Faculty of engineering, Hokkaido University, Japan*
Kita 13, Nishi 8, Kita-ku, Sapporo, Hokkaido, 060-8628, nawa@eng.hokudai.ac.jp

ABSTRACT

Investigations have been carried out to establish the electric characteristic and mass transport properties of hardened cement paste (HCP) by the AC impedance method. However, there are few studies considering the microstructure in HCP and the AC impedance method. In this study, the relationship between the electric conductivity measured by the AC impedance and microstructure in HCP was investigated, together with the effects of the moisture content in HCP on electric conductivity. Backscattered electron image analysis, the mercury intrusion method, and a water adsorption method were used to measure pore structure of the HCP. There was a strong correlation between relative humidity and the electric conductivity. It was shown that the electric conductivity is greatly influenced by the moisture content in HCP, at low relative humidities the conductivity is dependent on the surface area, and at high relative humidities the conductivity is dependent on the pore volume of the HCP.

Keywords. AC impedance, Pore structure, Electric conductivity, Moisture content, MIP

INTRODUCTION

Concrete is mainly composed of hardened cement paste (HCP) and aggregate, therefore, it is important to understand the transport properties of HCP to be able to predict the durability of a concrete to ensure the minimum environmental impact. The transport properties of HCP have been studied in much research (Kurumisawa, 2012), and one such non-destructive technique is the AC impedance method (Cabeza, 2002, Christensen, 1994, Gu, 1992, McCarter, 1990, 1988, Keddam, 1997). Investigations have been carried out for the electric characteristic and mass transport properties of HCP by the AC impedance method (Shi, 1999, McCarter, 2000), and evaluations of the durability of concrete by electric conductivity are simply conducted. However, it is well known that the electric conductivity changes with the ion concentration of the pore solution and by the drying of concrete (Johnson, 1988). The

effect of silica fume on the microstructure of hardened cement paste at different relative humidities has been reported (Rajabipour, 2007), as has the effect of drying on the electric conductivity (Tashiro, 1987, Wilkosz, 1995, McCarter, 1989, Saleem, 1996, Beaudoin, 2004). However, these studies did not report on the quantitative influence of drying on the conductivity and microstructure of hardened cement paste. In this study, the effect of the moisture content of HCP on electric conductivity was investigated, and the relationship between the electric conductivity measured by AC impedance and the microstructure of HCP was also investigated. Backscattered electron image analysis and the mercury intrusion method were used to determine the pore structure of HCP.

EXPERIMENTAL

Specimen preparation. Ordinary Portland cement (OPC) produced in Japan as shown in Table 1 was used. The water/cement ratios (0.3, 0.4, and 0.5) were used to produce a variety of microstructures in the hardened cement pastes. The specimens were cast in 40*40*10mm cubic molds for the electric conductivity measurements. The electrodes for the conductivity measurement were directly embedded in specimen apart from 30mm. The specimens were demolded after 24 h, and cured at 20 °C in saturated calcium hydroxide solution for 91days. After curing, the specimens were stored in sealed plastic containers at RH 11, 33, 43, 60, 74, 85, and 98% for more than 3months. The moisture content of specimen was determined by the weight loss between saturated and dried specimen after reached the equilibrium state.

Table 1. Physical and chemical properties of the cement

Density (kg/m^3)		3160		
Blaine surface area (cm^2/g)		3450		
Chemical composition (wt%)	SiO_2	20.83		
	Al_2O_3	5.59		
	Fe_2O_3	2.64		
	CaO	64.81		
	MgO	1.30		
	SO_3	2.02		
	TiO_2	0.25	Mineral composition of the cement by Bogue, calculated (%)	
	MnO	0.06		
	Na_2O	0.23	C_3S	58.4
	K_2O	0.50	C_2S	15.8
	P_2O_5	0.20	C_3A	10.4
	Cl	0.021	C_4AF	8.03

X-ray diffraction (XRD) measurements. Samples for measurement were powder that was crushed by ball mill and mixed with 10%wt of corundum (Al_2O_3) as an internal standard. The conditions of the XRD measurements were 40kV, 40mA, and CuKα X-rays monochrometer attached. The Rietveld method was used for the quantitative analysis of the

composition of the hydrated cement (C_3S, C_2S, C_3A, C_4AF, AFm, Aft, and CH), and was performed with Siroquant software.

Backscattered electron image (BEI) measurements. Five mm cubes were cut from the freeze-dried samples of the hardened cement pastes and used for the BEI observations. The dried specimen cubes were immersed in epoxy resin in a vacuum; after the hardening of the epoxy resin, a specimen surface was polished using SiC paper, and finally smoothed by 0.25 micrometer diamond paste, and a carbon coat was applied to provide electric conductivity on the specimen surface. The electron microscopy imaging was conducted under the following conditions: an acceleration voltage of 15 keV, a working distance of 17 mm, a field size of 200 × 150 μm, and a pixel size of 0.32 μm. The resulting resolution in this study is 0.32 μm, and it was not possible to distinguish pores narrower than 0.32 μm in diameter. Observations were carried out on 16 fields in each specimen. Unhydrated cement (UH), unhydrated slag, calcium hydroxide (CH), C-S-H (including fine pores and other hydrates), and pores larger than 0.32 μm were distinguished using image analysis software and setting brightness thresholds. The average area fraction of each phase was considered to be the volume fraction (Igarashi, 2004, Scrivener, 2004).

Mercury intrusion porosimetry (MIP). Crushed freeze dried sample (2.5-5.0mm) was used for the MIP. The porosity and pore size distribution determination was carried out by a mercury intrusion porosimeter capable of generating pressure in the range from subambient to 33,000 psi (227 MPa). The pore radius calculations were performed with the Washburn equation.

BET surface area of the hydrated cement paste. The BET surface area of the hydrated cement paste was measured with the water vapour isotherm (Hydrosorb1000, Quantachrome). The sample for the measurements was powder that had been crushed with a ball mill and dried by freeze-drying. Sample was placed in a vacuum at 105 degrees Celsius for 1hour before the measurements, and measurements were at 0.05-0.98 relative pressure. The surface area was determined from an adsorption curve established by the multi points BET method.

The electric conductivity. The size of the specimens for the electric conductivity measurements was 40*40*10mm, the stainless electrodes (5*30*0.3mm) were placed 30 mm apart on the specimens (Figure 1). The effective area of the electrode is 5*30mm, and the

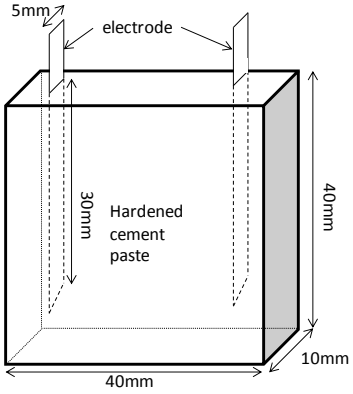

Figure 1. Schematic of specimen for the conductivity measurement

AC impedance of the specimens was measured from 4Hz to 5MHz with an impedance analyzer (HIOKI IM3570). After the measurements a Nyquist plot (Z': real axis, Z":imaginary axis) was established from the acquired data, and the bulk resistivity was determined from the point where two parts of the electrode resistivity curve (straight line and curved) reaches the minimum as shown in Figure 2.

$$R_t = \frac{R_a L}{A} \tag{1}$$

$$\sigma = \frac{1}{R_t} \tag{2}$$

with Rt: the bulk resistivity of specimen, Ra: the measured resistivity, L: the distance between electrodes, A: the effective area of the electrode, and σ: the conductivity. The electric conductivity of hardened cement paste depends on the porosity, pore connectivity, and conductivity of the pore solution in the hardened cement paste (Snyder, 2003). The influence of concentration of the pore solution was not considered it in this study.

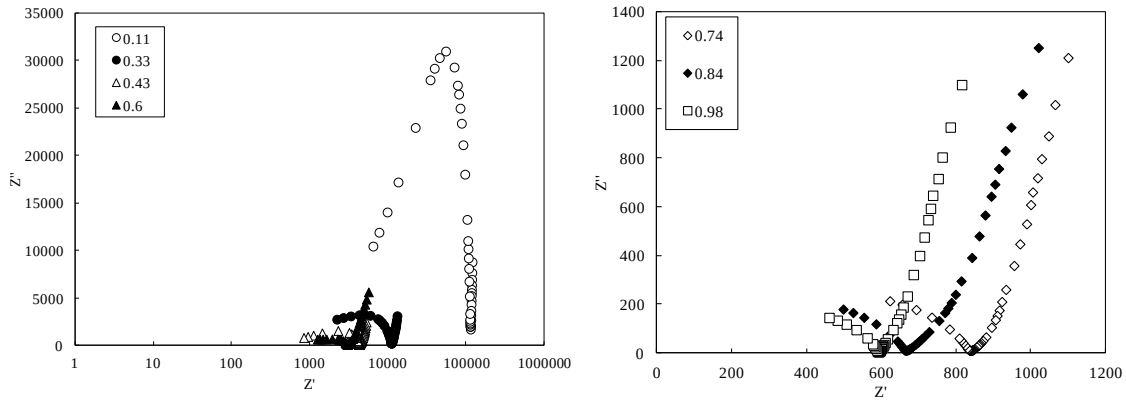

Figure 2. Nyquist plot of hardened cement paste (left: low relative humidities (0.11-0.6, right: high relative humidities (0.74-0.98), W/C 0.5)

RESULTS

BEI observations. Figure 3 shows the backscattered electron image of the hardened cement paste, black, dark grey, light grey, and white pixels show pores, C-S-H, CH, and UH, respectively. As the water to cement ratio increases, there were more large capillary pores, showing that specimens with higher water to cement ratios have a more porous structure. The results show that it was possible to produce hardened cement pastes with different microstructures. The area fractions of each phase calculated from the BEI images are shown in Figure 4, for each specimen showing the average of 16 BEI images. The unhydrated cement decreased with increases in the water to cement ratios, and CH increased with increases in the water to cement ratios.

XRD measurements. The XRD profiles of hardened cement paste powders are shown in Figure 5. The peak heights of calcium hydroxide (CH) and monosulfate (AFm) varies with the water to cement ratio. The composition of the hydrated cement paste calculated by Rietveld method is shown in Figure 6. The amount of calcium hydroxide increases with increases in the water to cement ratio as shown in Figure 4 calculated from BEI. Both Figure 4 and 6 quantitatively shows that major part of the hardened cement paste is C-S-H.

BET surface area measurements. The results of the BET surface area measurements are shown in Table 2. The surface area of the hardened cement paste decreases with increases in the water cement ratio. Mikhail reported that the surface area was around 200m^2/g in all cement pastes (Mikhail, 1964), but the value in our study is lower, because surface area is strongly influenced by curing age and pre-treatment of the specimen as shown in previous reports.

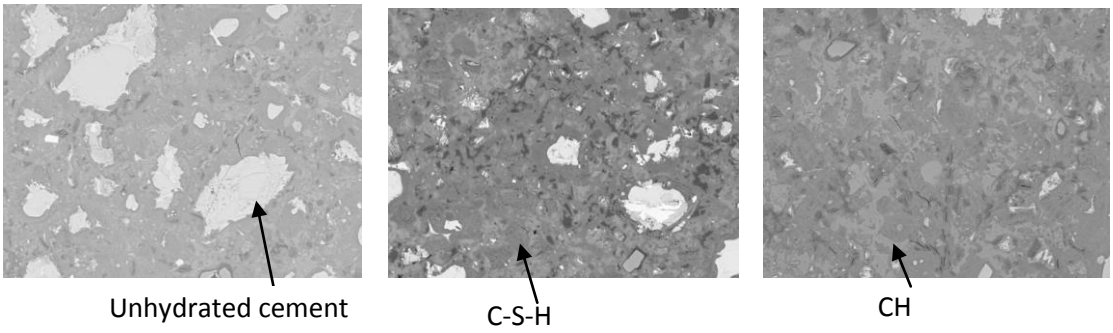

Figure 3. BEI of different W/C hardened cement pastes (curing age: 91day, image size: 200*150μm)

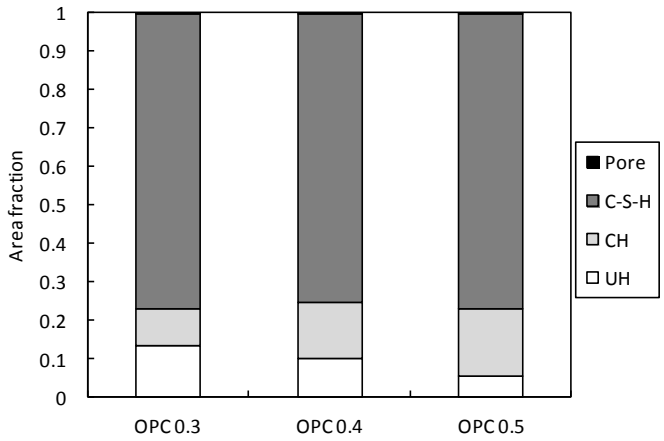

Figure 4. Area fractions of each phase in the hardened cement paste calculated from the BEI images

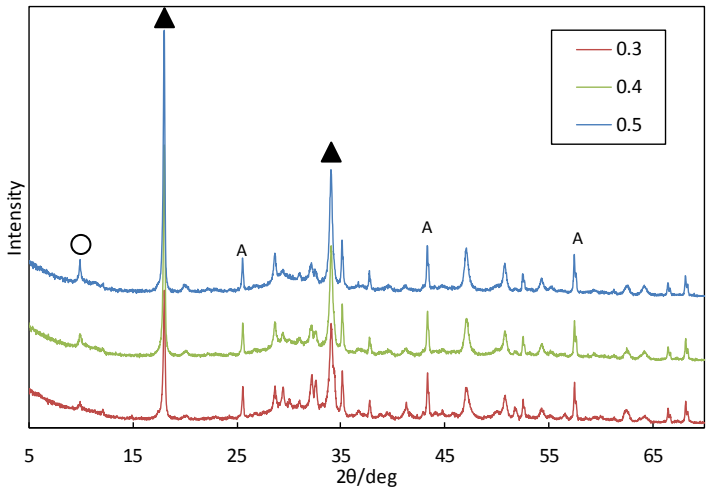

Figure 5. XRD profiles of hardened cement paste (▲:CH, ○:AFm, A:Al_2O_3)

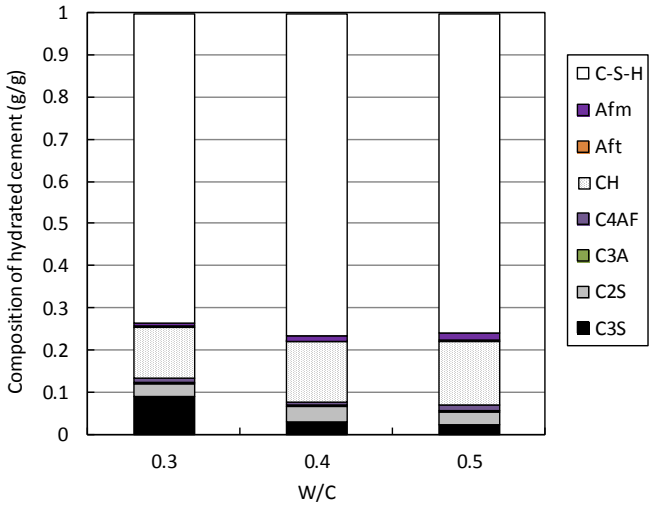

Figure 6. Composition of hardened cement pastes calculated by the Rietveld method

Table 2. BET surface areas measured by the H_2O isotherm

W/C	BET surface area (m^2/g)
0.3	134.6
0.4	127.8
0.5	120.4

MIP measurements. The MIP results are shown in Figure 7. Most of the pores in all of the specimens are narrower than 0.1μm in pore diameter. The pore volume increased with increases in the water to cement ratio. The threshold pore diameter of W/C 0.5 was a largest, the value was 0.03μm.

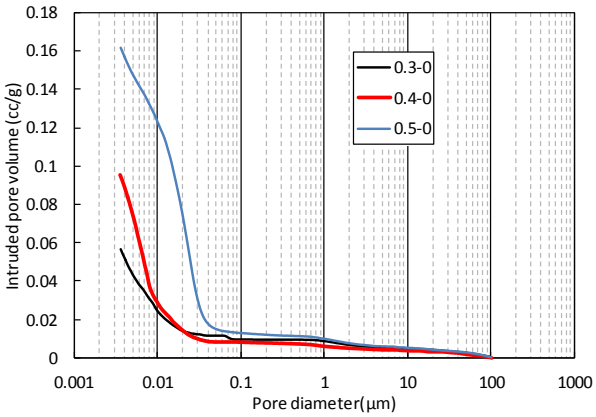

Figure 7. Pore volume in hardened cement pastes measured by MIP

The electric conductivity measurements. The electric conductivity determined from Figure 2 increases with different relative humidities as shown in Figure 8. Above the R.H. 0.6 the electric conductivity is higher for higher the water to cement ratios, but for relative humidities below 0.6 the electric conductivity was higher for lower the water to cement ratios. The influence of the surface conduction varied according to a water to cement ratio, but surface conduction at R.H. 11% was in a very low range, from 1/1000 to 1/100 of the saturation condition, and the influence of the surface conduction can be ignored at the saturation condition as shown in previous report (Rajabipour, 2007). The relation of the electric conductivity and moisture content is shown in Figure 9. The electric conductivity increases with the moisture content, and the moisture content influences on the electric conductivity strongly. This shows that the relation between the moisture content and electric conductivity was determined by exponential functions, however, the correlation coefficient is low due to the effect of pore solution conductivity.

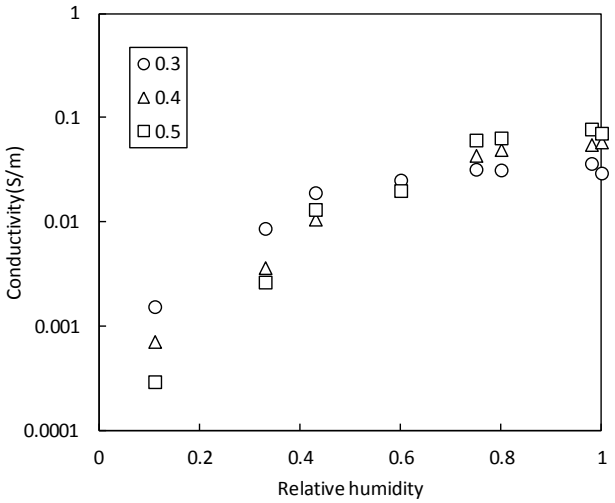

Figure 8. The electric conductivity of hardened cement pastes at different relative humidities

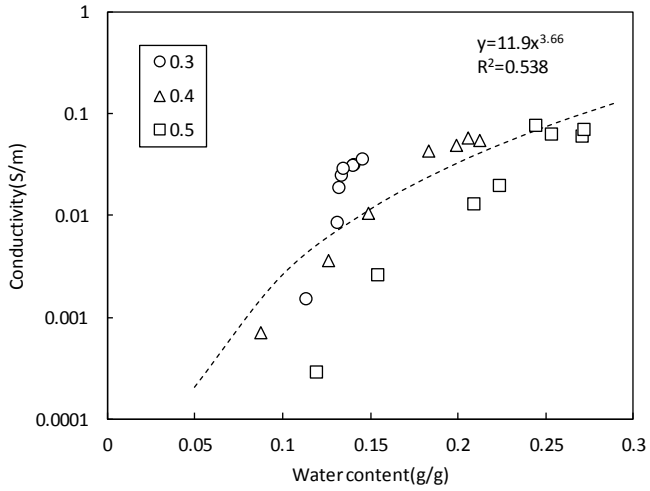

Figure 9. Plot of the electric conductivity vs. the moisture content of the hardened cement pastes

DISCUSSION

At the saturation condition, the electric conductivity of porous media is a function of pore volume as shown by Archie's law. In this section, the effect of the microstructure of the hardened cement paste on electric conductivity at different humidities is discussed. The results of the electric conductivity and pore volume or BET surface area measurements at different relative humidities are shown in Figure 10. The electric conductivity of all of the specimens increased with high pore volume (left figure) at high relative humidities, but at low humidities it decreased with pore volume. The relation between BET surface area and electric conductivity (right figure), the electric conductivity decreased with high surface area at high relative humidities, but at low humidities it increased with surface area. Taken together this suggests that at high relative humidities the electric conductivity is influenced by pore volume (pore solution), and at low relative humidities the electric conductivity is influenced by the surface area. This makes it essential to consider the influence of the humidity in electric conductivity measurements. For R.H 0.11-0.33, the statistical thickness of water adsorption that was calculated by the H_2O adsorption isotherm is from 0.23nm to 0.4nm. That is implying the transport of ions occurred in monolayers of H_2O molecules. In addition, the effect of the pore volume (pore solution) and the surface area on electric conductivity is expressed as the following equation (Nettelblad, 1995, Waxman, 1968),

$$\sigma_{eff} = \frac{1}{F}\left(\sigma_w + \frac{2\sigma_{surf}}{\Lambda}\right) \tag{3}$$

where, σ_{eff}: effective electric conductivity, F: formation factor, σ_w: pore solution conductivity , σ_{surf}: surface conductivity, and $2/\Lambda$: the surface to volume ratio of the pores. From this equation, when the pore solution is fully evaporated, the electric conductivity is proportional to the surface area. When the measurement of the electric conductivity is carried out at the low humidities, this influence of the surface area conduction is not negligible and must be considered.

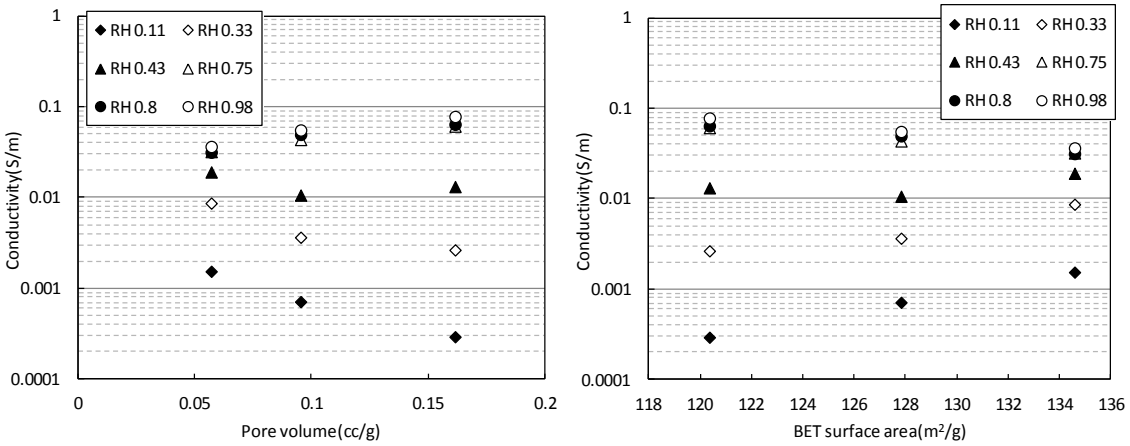

Figure 10. Relationship between the electric conductivity, and pore volume (left) or BET surface area (right) of hardened cement paste with different relative humidity

CONCLUSIONS

This paper elucidates the influence of drying and microstructure on the electric conductivity of hardened cement pastes. The electric conductivity decreases with drying. The influence of drying on the electric conductivity was suggested to be a function of moisture content. It was shown that the electric conductivity was greatly influenced by the moisture content in hardened cement paste. And it was quantitatively shown that the electric conductivity of hardened cement paste depended on the surface area at low relative humidities and on the pore volume at high relative humidities. When durability of concrete structures is evaluated by electric conductivity, it was further established that it is necessary to consider the influence of the humidity when determining the electric conductivity.

ACKNOWLEDGMENT

We thank the Ministry of Education, Culture, Sports, Science and Technology for financial support with the research here.

REFERENCES

Beaudoin, J.J., Tamtsia, B.(2004). “Effect of drying methods on microstructural changes in hardened cement paste: an a.c. impedance spectroscopy evaluation.” Journal of Advanced Concrete Technology, 2 (1), 113–120.

Cabeza, M., Merino, P., Miranda, A., Nóvoa, X.R., Sánchez, I. (2002). “Impedance spectroscopy study of hardened portland cement paste.” Cem. Concr. Res., 32, 881–891.

Christensen, B.J., Coverdale, R.T., Olson, R.A., Ford, S.J., Garboczi, E.J., Jennings, H.M., Mason, T.O. (1994). “Impedance spectroscopy of hydrating cement-based materials: measurement, interpretation, and application.” J. Am. Ceramic. Soc., 77(11), 2789–

2802.
Gu, P., Xie, P., Beaudoin, J. J., Brousseau, R. (1992). “AC impedance spectroscopy (I): A new equivalent circuit model for hydrated portland cement paste.” Cement and Concrete Research, 22(5), 833–840.
Igarashi, S. Kawamura, M. Watanabe, A. (2004). “Analysis of cement pastes and mortars by a combination of backscatter-based SEM image analysis and calculations based on the Powers model.” Cement and Concrete Composites, 26(8), 977–985.
Johnson, D.L., Sen, P.N. (1988) “Dependence of the conductivity of a porous medium on electrolyte conductivity.” Physical Review B 37(7), 3502–3510.
Keddam, M., Takenouti, H., Novoa, X. R., Andrade, C. (1997). “Impedance measurements on cement paste.” Cement and Concrete Research, 27(8), 1191–1201.
Kurumisawa, K., Nawa, T., Owada, H. (2012). “Prediction of the diffusivity of cement-based materials using a three-dimensional spatial distribution model.” Cement and Concrete Composite, 34(1), 408-418.
McCarter, W.J., and Garvin, S. (1989). “Dependence of electrical impedance of cement-based materials on their moisture condition.” J. Phys.D: Appl. Phys., 22, 1773-1776.
McCarter, W.J., and Brousseau, R. (1990). “The A.C. response of hardened cement paste.” Cement and Concrete Research, 20(6), 891–900.
McCarter, W. J., Garvin, S. and Bouzid, N. (1988). “Impedance measurements on cement paste.” Journal of Materials Science Letters, 7(10), 1056-1057.
McCarter, W.J., Starrs, G., Chrisp, T. M. (2000). “Electrical conductivity, diffusion, and permeability of Portland cement-based mortars.” Cem. Concr. Res., 30(9),1395–1400.
Mikhail, R. S., Copeland, L. E., Brunauer, S. (1964). “Pore structures and surface areas of hardened Portland cement pastes by nitrogen adsorption.” Canadian Journal of Chemistry, 42(2), 426-438.
Nettelblad, B., Ahlen, B., Niklasson, G.A., Holt, R.M. (1995). “Approximate determination of surface conductivity in porous media.” J Phys D 28(10), 2037–2045
Rajabipour, F., Weiss, J. (2007). “Electrical conductivity of drying cement paste.” Materials and Structures, 40(10), 1143-1160.
Saleem, M et al. (1996) “Effect of moisture, chloride and sulphate contamination on the electrical resistivity of Portland cement concrete.” Construction and Building Materials, 10(3), 209-214.
Scrivener, K, L. (2004). “Backscattered electron imaging of cementitious microstructures: understanding and quantification.” Cem. Concr. Comp., 26(8), 935–945.
Scuderi, C.A., Mason, T.O., Jennings, H.M. (1991) “Impedance spectra of hydrating cement pastes.” Journal of materials science, 26(2), 349-35.
Shi, M., Chen, Z., Sun, J. (1999). “Determination of chloride diffusivity in concrete by AC impedance spectroscopy.” Cem. Concr. Res., 29, 1111–1115.
Snyder, K.A., Feng, X., Keen, B.D., Mason, T.O. (2003). “Estimating the electrical conductivity of cement paste pore solutions from OH−, K+, and Na+ concentrations.” Cement and Concrete Research, 33(6), 793–798.
Tashiro, C. and Shimamura, H. (1987). “Dependence of the electrical resistivity on evaporable water content in hardened cement pastes.” Materials Science Letter,(6), 1379.
Waxman, M .H., and Smits, L.J.M. (1968). “Electrical conductivity oil-bearing shaly sands. ” Soc. Pet. Eng. J. , 8, 107-122
Wilkosz, D.E., and Young, J.F. (1995). “Effect of moisture adsorption on the electrical properties of hardened Portland cement compacts.” J. Am. Ceram. Soc., 78(6), 1673-1679.